5ème Conférence Internationale des Energies Renouvelables (CIER– 2017)
Proceeding of Engineering and Technology –PET
Vol.28 pp.87-92

Enhancement design and performance comparative analysis of hydrogen based thermally driven absorption refrigeration cycles for solar cooling

N. BEN EZZINE [#,*1], M. CHATTI [#], R. GARMA [#], A. BELLAGI [#2]

[#] *U.R. Thermique et Thermodynamique des Procédés Industriels,*
Ecole Nationale d'Ingénieurs de Monastir, Av. Ibn Jazzar, 5060 Monastir, Tunisia
[1] n_benezzine@yahoo.fr
[2] a.bellagi@enim.rnu.tn
[*] *Faculté des Sciences de Bizerte,*
Université de Carthage, 7021 Zarzouna, Tunisia

***Abstract*— Solar thermally driven cooling systems offers a more sustainable and low-energy solution for refrigeration and air-conditioning applications. The common basic configuration of hydrogen diffusion absorption refrigerator BHDAR is the Pluten-Munters invented in the 1920s and manufactured by Electrolux (today Dometic AB).**
In this study three hydrogen-ammonia-water diffusion absorption cycles with increasing internal heat recovery have been investigated and compared by numerical simulation.
Simulations are performed for two cooling medium temperatures, 27°C and 35°C, and four driving heat temperatures in the range [90°C - 180°C]. The performance characteristics are analyzed parametrically by computer simulation. Results show that the system performance and the lowest (minimum) evaporation temperature reached are largely dependent upon the absorber efficiency and the maximum driving temperature.
The second novel enhanced MHDAR2 cycle reaches a maximum COP of 0.38 and minimum evaporation temperature of -24°C in the air cooled case. While for the same conditions, the conventional BHDAR cycle COP cannot exceed 0.22 with a generator driving temperature of about 140°C.

***Keywords*— Modelling, Simulation, COP, Absorption, Refrigeration, Coefficient of performance, Enhancement design, heat recovery**

I. INTRODUCTION

In recent years, research has been devoted to improvement of absorption refrigeration systems. Mechanical vapour compression refrigerators have been used in many refrigeration and air-conditioning applications. However, increased global warming and environmental effect of chlorofluorocarbon has stimulated interest in the development of absorption refrigeration.

Hydrogen Diffusion absorption refrigeration (HDAR) cycle invented by the Swedish engineers von Platen and Munters [1] has been recognized as one of the most promising technologies for refrigeration and cooling production. The corresponding thermodynamic cycle is based on refrigerant/absorbent pair mixture as working fluids and an inert gas for pressure equalization. A thermally driven bubble pump, which can be powered by solar thermal energy, is used to lift the liquid solution. As a result of the absence of any mechanical moving part, the refrigerator is silent and very reliable [2] in addition of an economical and natural relative cycle.

Over the years, numerous researches in this field have been done and a lot more is still undergoing. Works were mainly focused on thermodynamic modelling, finding new working fluids and improving the heat and mass transfers in mainly components of the HDAR. Ben Ezzine et al. [10] presented an experimental investigation of an air-cooled diffusion absorption machine operating with a binary light hydrocarbon mixture (C_4H_{10}/C_9H_2O) as working fluids and helium as pressure equalizing inert gas. They produced cold at temperatures between −10 and +10 °C for a driving temperature in the range of 120–150 °C. Zohar et al. [11] examined numerically the performance of a HDAR system working with an organic absorbent (DMAC-dimethylacetamide) and five different refrigerant which were chlorodifluoromethane (R22), difluoromethane (R32), 2-chloro-1,1,1,2-tetrafluoroethane (R124), pentafluoroethane (R125) and 1,1,1,2-tetrafluoroethane (R134a) and helium as inert gas. They compared performance results of their systems with the performance of the same system working with ammonia–water and helium. They found out that similar behavior for all systems, regarding the coefficient of performance (*COP*) and rich and poor solution concentrations as functions of generator temperature. Ben Ezzine et al. [12] investigated the feasibility of a HDAR operating with the working fluid system DMAC-R124 and coupled to a solar collector. The performance characteristics of this system were found by a computer simulation. They showed that the *COP* and the produced cold temperature depend largely on the effectiveness of the absorber and on the generator temperature. The results indicated that at the same driving temperature (140 °C), the *COP* of the HDAR system working with R124-DMAC was equal to 0.32 (maximum value) that was approximately 50% higher than that of the ammonia water refrigerator. Moreover, the lowest evaporation temperature was obtained as −14.8 °C at the driving temperature of 180 °C.

ISSN 2356-5608

Most of the work on hydrogen diffusion absorption refrigerators reported in the literature involves thermodynamic modelling and looking for new fluids associated or not to experimental tests. However few research has been performed on theoretical and practical enhancement design of the basic conventional HDAR. The present paper is a contribution to enhancement and research for new enhanced HDAR configurations. Numerical investigations are then performed for three studied hydrogen-ammonia-water cycles with hydrogen as the auxiliary gas. The effects of different operating parameters on the system performances are analysed and discussed.

II. Description of the HDAR cycle

The conventional Hydrogen Diffusion Absorption system shown in Figure 1 is the Platen-Munters HDAR (Basic Hydrogen Diffusion Absorption Refrigerator) manufactured by Electrolux. It includes an absorber, an evaporator-gas heat exchanger, a rectifier, a condenser, a solution heat exchanger and a generator where the boiler and the bubbles pump are combined. It relies on a bubble pump to pump the solution from the lower level to the higher one.

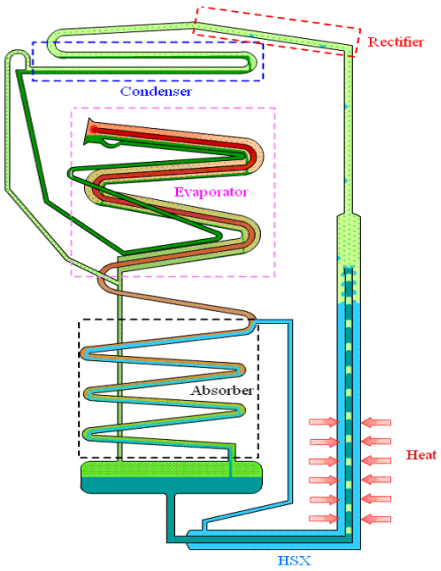

Fig. 1 Schematic representation of view of the Platen-Munters HDAR

The BHDAR may be simplified on a schematic diagram as shown in Figure 2. The rich solution (6) leaving the absorber flows to the generator where it is heated causing the evaporation of some ammonia refrigerant. The resulting vapor bubbles rise in the tube. These vapor bubbles, which are separated by small liquid slugs, occupy the complete cross-section of the tube due to its small diameter. Each bubble acts as a gas piston and lifts the corresponding liquid slug to the top of the pump tube. Under the effect of the difference in height between the top of the bubble pump tube and the top of the absorber, the weak solution (8) flows to the absorber via a solution heat exchanger SHX. Usually the vapor leaving the generator (10) contains a quantity of absorbent (H_2O). This vapor is then purified in the rectifier. The ammonia vapor (1) is then liquefied in the condenser. The liquid refrigerant (2) passes to the evaporator top. Since the evaporator is charged with hydrogen, the partial pressure of refrigerant decreases. It results that the ammonia evaporates at law temperature. As long as the refrigerant continues to evaporate, its partial pressure is rising. The resulting NH_3/Hydrogen vapor mixture (5) flows out of the evaporator into the absorber which is continuously cooled and where the NH_3 weak solution absorbs the NH_3 from the vapor phase and forms an NH_3/H_2O rich solution (6).

The HDAR is a self circulate system. The solely circulation is due to the gravity and density difference between the components working fluid.

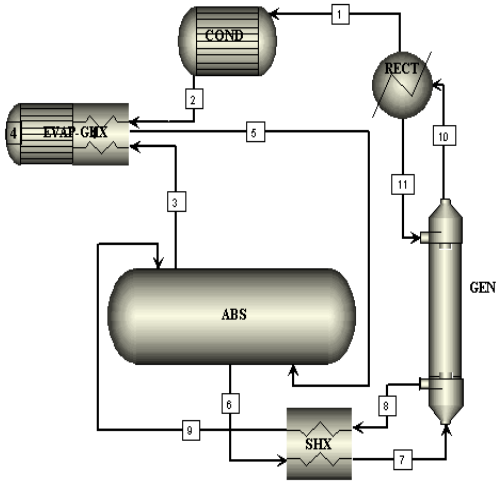

Fig. 2 Circulation patterns of the Basic Hydrogen Diffusion Absorption Refrigerator BHDAR

III. Modelling and simulation

A numerical model should be developed first. The modeling proceeds by formulation of the mass and energy balances, specification of the fundamental operating conditions, characterization of the heat and mass transfer processes in the various heat and mass exchanging devices and specification of the state of the working fluid and operating conditions at several locations of the installation. Thermodynamic properties of working fluids are calculated in a subroutine incorporated in the main program [20-23].

Generator

Total mass balance, ammonia mass balance, and energy balance of the HDAR generator are expressed as follows:

$$\dot{m}_7 + \dot{m}_{11} = \dot{m}_8 + \dot{m}_{10} \quad (1)$$

$$\xi_r.\dot{m}_7 + \xi_{11}.\dot{m}_{11} = \xi_w.\dot{m}_8 + \psi_{10}.\dot{m}_{10} \quad (2)$$

$$\dot{Q}_{Gen} + \dot{m}_7.H_7 + \dot{m}_{11}.H_{11} = \dot{m}_8.H_8 + \dot{m}_{10}.H_{10} \quad (3)$$

The weak solution temperature T_8 leaving the generator is the highest temperature in the cycle. The leaving liquid solution and the vapour are in saturated state and at the same temperature, i.e.

$$T_8 = T_{10} \quad (4)$$

Absorber

Total mass balance, ammonia mass balance, and the heat released by the exothermic process and rejected to the environment medium are expressed as follows:

$$\dot{m}_{5,H2} = \dot{m}_{3,H2} \quad (5)$$

$$\dot{m}_{5,NH3} + \dot{m}_9 = \dot{m}_{3,NH3} + \dot{m}_6 \quad (6)$$

$$\dot{m}_{5,NH3} + \xi_w.\dot{m}_9 = \dot{m}_{3,NH3} + \xi_r.\dot{m}_6 \quad (7)$$

$$\dot{Q}_{Abs} + \dot{m}_6.H_6 + \dot{m}_{3,NH3}.H_{3,NH3} + \dot{m}_{3,H2}.H_{3,H2} = \dot{m}_9.H_9 + \dot{m}_{5,NH3}.H_{5,NH3} + \dot{m}_{5,H2}.H_{5,H2} \quad (8)$$

Since the condenser has the same cooling medium, we assume that the same temperature difference prevails between the cooling medium and the exiting condensate, i.e.

$$T_9 = T_2 = T_C + \Delta T_{Cond} \quad (9)$$

The ammonia rich solution (9) leaving the absorber is in sub-cooled state.

To characterize absorption process absorber effectiveness is defined as the ratio between the quantities of refrigerant absorbed to the maximum refrigerant quantities that can be absorbed in the same operating conditions.

$$Eff^G_{Abs} = \frac{\dot{m}_{5,NH3} - \dot{m}_{3,NH3}}{\dot{m}_{5,NH3} - (\dot{m}_{3,NH3})_{min}} \quad (10)$$

$$Eff^L_{Abs} = \frac{\xi_r.\dot{m}_6 - \xi_w.\dot{m}_9}{\xi_{rMax}.\dot{m}_{6Max} - \xi_w.\dot{m}_9} \quad (11)$$

Where $\xi_{rMax}, \dot{m}_{6Max}$ and $(\dot{m}_{3,NH3})_{min}$ are defined as the thermodynamic limits of the absorption process in the bottom and top of the absorption column. In fact, $\xi_{rMax,}$ is the highest NH_3 mass fraction that can be contained in the rich solution and which can be reached when the thermodynamic equilibrium in the absorber's bottom is established at the partial pressure of the refrigerant leaving the evaporator. In such condition mass flow rate of the rich solution reaches its maximum value $\dot{m}_{6Max}$, finally $(\dot{m}_{3,NH3})_{min}$ is the lowest mass flow rate of the NH_3 residual in the gas mixture leaving the top the absorber and which can be reached when the gas mixture is in equilibrium with the weak solution (9) at the same temperature.

Evaporator-gas heat exchanger

Contrary to conventional two pressure absorption refrigeration systems when refrigerant is evaporated at constant evaporation low pressure, the evaporation process in hydrogen based triple fluid diffusion absorption refrigeration system is effectuated between two refrigerant partial pressure. At the evaporator entrance, the sub-cooled liquid refrigerant (2) leaving the condenser at the total system pressure arrives at the evaporator entrance, relaxes into the hydrogen and NH_3 mixture and the result is that the partial pressure of the sub-cooled liquid NH_3 drops and it starts to evaporate at low temperatures. More the liquid evaporates while traversing the evaporator more the refrigerant partial pressure in the vapor phase increases. Therefore temperature through the evaporator-gas heat exchanger increases and the evaporator-gas heat exchanger outlet temperature T_5 is then fixed.

Many factors affect the evaporation process such as refrigerant mass flow, NH_3 partial pressure, temperature, absorber effectiveness, etc. The partial pressure of NH_3 in the gas mixture is defined as:

$$P_{Part} = \frac{\dot{n}^g_{NH3}}{\dot{n}^g_{NH3} + \dot{n}_{H2}} * P_{Syst} \quad (12)$$

$$P_{PartMax} = \frac{\dot{n}^g_{5,NH3}}{\dot{n}^g_{5,NH3} + \dot{n}_{5,H2}} * P_{Syst} \quad (13)$$

$$P_{PartMin} = \frac{\dot{n}^g_{3,NH3}}{\dot{n}^g_{3,NH3} + \dot{n}_{3,H2}} * P_{Syst} \quad (14)$$

The lowest temperature attempted in the evaporator's top can be calculated when $P_{PartMin}$ is known. Total mass balance, ammonia mass balance, and energy balance on the HDAR evaporator are expressed as follows:

$$\dot{m}_{5,H2} = \dot{m}_{3,H2} \quad (15)$$

$$\dot{m}_{3,NH3} + \dot{m}_2 = \dot{m}_{5,NH3} \quad (16)$$

$$\dot{Q}_{Evap} + \dot{m}_2.H_2 + \dot{m}_{3,NH3}.H_{3,NH3} + \dot{m}_{3,H2}.H_{3,H2} = \dot{m}_{5,NH3}.H_{5,NH3} + \dot{m}_{5,H2}.H_{5,H2} \quad (17)$$

A. HDAR performances

Coefficient of performance is defined as:

$$COP = \frac{\dot{Q}_{Evap}}{\dot{Q}_{Gen}} = \frac{\dot{Q}_{Evap}}{\dot{Q}_B + \dot{Q}_{BP}} \quad (18)$$

The theoretical reversible cycle is assumed to operate between three thermal sources, a cold source at $T_F = T_4 = T_{Min}$, a medium source at T_C and a driving heat source at $T_G = T_8$. The theoretical *COP* is then expressed:

$$COP_{rev} = \frac{T_F(T_G - T_C)}{T_G(T_C - T_E)} \quad (19)$$

The cycle efficiency writes:

$$\eta = \frac{COP}{COP_{rev}} \quad (20)$$

The circulation ratio is defined as the ratio between the rich solution mass flow rate and that of the refrigerant:

$$f = \frac{\dot{m}_6}{\dot{m}_1} \quad (21)$$

B. Numerical resolution

The simulation model, performed later on a well designed computer code, is constituted of a large set of non-linear equations (mass and energy balances and thermodynamic properties equations) which is simultaneously solved using a FORTRAN program coding the CONLES algorithm [23, 24].

IV. Simulation Results and Discussion

The thermodynamic properties of the NH_3/H_2O solution at various locations of the cycle are calculated in the basis of the correlations between P-T-x–y for the liquid phase and vapor phases and the h-x-T diagram correlations [20, 21].

The cycle is simulated with two cooling medium temperatures, 27°C for water-cooling and 35°C for air-cooling. For each cooling medium temperature the cycle is simulated with three driving temperature 90°C, 120°C and 140°C for water-cooled cycle and 120°C,140°C and 180 °C for air-cooled machine. The most important calculation results of the BHDAR cycle for the two cases presented in table 1 provides the exchanged heat rates, the circulation ratio and the coefficient of performance of the various configurations. We notice that in the case of water cooling, driving heat temperatures above 120°C are not necessary, unlike the case of air cooling where higher temperatures are needed to enhance the coefficient of performance.

Based on the simulated results, the thermodynamic cycle of the air-cooled HDAR is represented on the NH_3/H_2O OLDHAM diagram shown in figure 3. In this figure, real values of temperatures, mass concentrations, and partial pressure of different HDAR's components respect the points' state referenced to figure 2. The transformation (2-4) represents the refrigerant relaxation caused by the presence of hydrogen in the evaporator inlet and the transformation (4-5-6) corresponds to the NH_3 evaporation process inside the evaporator.

TABLE I

BASE CASE SIMULATION RESULTS: HEAT EXCHANGE RATES AND PERFORMANCES OF THE MACHINE.

Parameter \ T_{Max}	Water cooled, T_C = 27 °C			Air cooled, T_C = 35 °C		
	90°C	120°C	140°C	120°C	140°C	180°C
$\dot{Q}_{Evap}$ (W)	1000.	1000.	1000.	1000.	1000.	1000.
$\dot{Q}_{Gen}$ (W)	3964.	2767.2	3222.6	6104.7	4554.8	7517.
$\dot{Q}_{Abs}$ (W)	2119.2	1604.2	1623.4	2616.6	2026.7	1998.9
$\dot{Q}_{Cond}$ (W)	2357.4	1454.8	1386.4	3155.9	2037.7	1731.8
$\dot{Q}_{Rect}$ (W)	487.3	708.2	1212.6	1332.2	1490.3	4786.2
f	9.27	4.1	3.29	6.95	4.56	3.12
COP	**0.252**	**0.361**	**0.31**	**0.163**	**0.22**	**0.133**

V. System Parameters Effect on Performance

Figure 4 represents the evolution of the base case air cooled HDAR coefficient of performance vs. the driving heat temperature for different absorber efficiencies. It shows that for constant absorber efficiency the COP increases first to a maximum value with increasing temperature and then diminishes. On the other hand, the performance of the installation is largely affected by the absorber efficiency: it diminishes sharply when the efficiency gets lower. Some cycle parameters are influenced by the driving temperature variation.

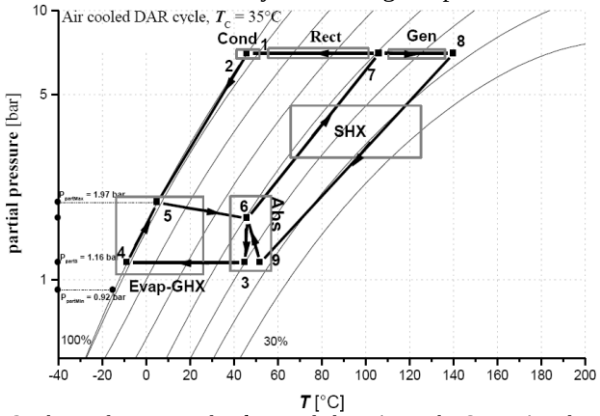

Fig. 3: Thermodynamic cycle of air cooled HDAR in the OLDHAM diagram

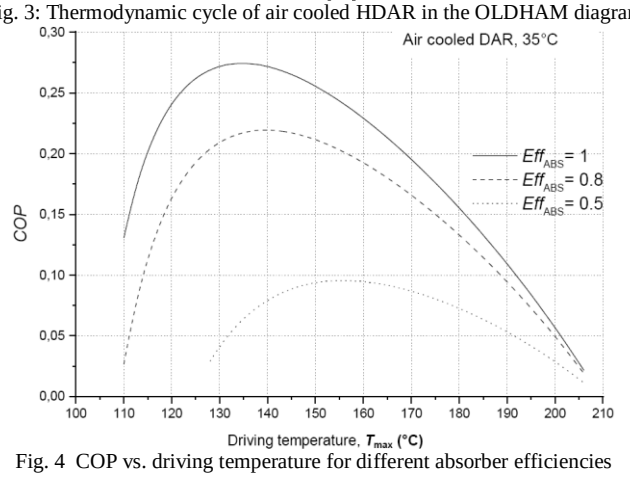

Fig. 4 COP vs. driving temperature for different absorber efficiencies

The dependency of the minimum evaporation temperature, T4, in the air cooled DAR on the driving temperature and the absorber effectiveness is also studied and depicted in figure 5. It can be clearly observed that the minimum evaporation temperature decreases by increasing the driving temperature. It is also found that the higher absorber effectiveness, the lower T4, i.e. that more refrigerant NH3 is absorbed by the weak solution.

VI. First Enhanced Modified Cycle, MHDAR1

This new enhanced configuration of HDAR shown in figure 6, is an extension of the standard BHDAR composed of a condenser, an evaporator/gas heat exchanger, an absorber, a solution heat exchanger, a generator and an external cooled rectifier.

The higher the temperature of the driving source increases more rectifier losses to the external cooling environment are more interesting. For recovering of this amount of energy lost

a new internal rectifier is then integrated between absorber and the solution heat exchanger SHX. The amount heat generated by the rectification effect is then is then recovered by rich ammonia solution (6) leaving the bottom of the absorber. The obtained preheated rich solution (12) through the rectifier is then mixed with the liquid reflux (11) at the mixer. New rich ammonia mixture (13) leaving the mixer is forwarded to generator bubble pump via the solution heat exchanger (SHX) as presented in figure 6.

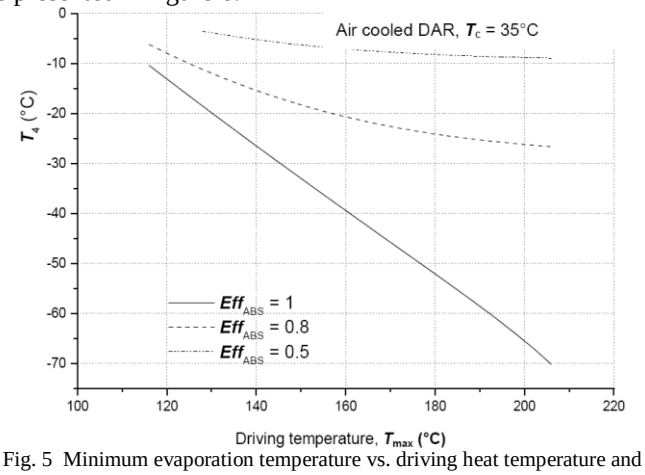

Fig. 5 Minimum evaporation temperature vs. driving heat temperature and absorber efficiency

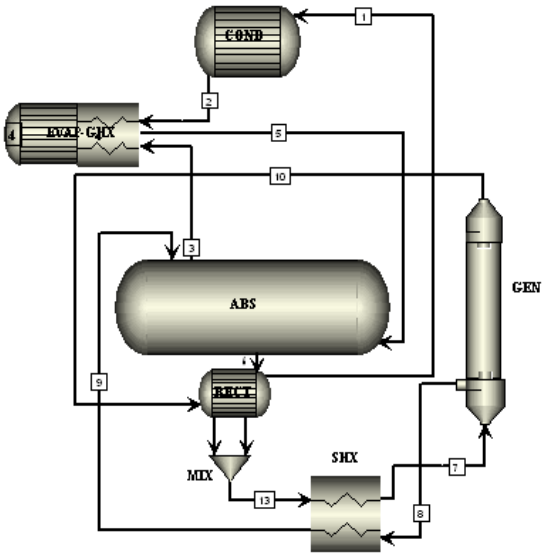

Fig. 6 Circulation patterns of the MHDAR1

Figure 7 reports the results of the comparison between the basic BHDAR and the first enhanced modified MHDAR1 performance in air cooled case for varying driving heat temperatures. It shows clearly that MHDAR1 is more performing. The COP is at maximum with a value of 0.24 with a driving temperature of 140°C, that is higher than that of the BHDAR operating in the same conditions.

VII. SECOND ENHANCED MODIFIED, MHDAR2

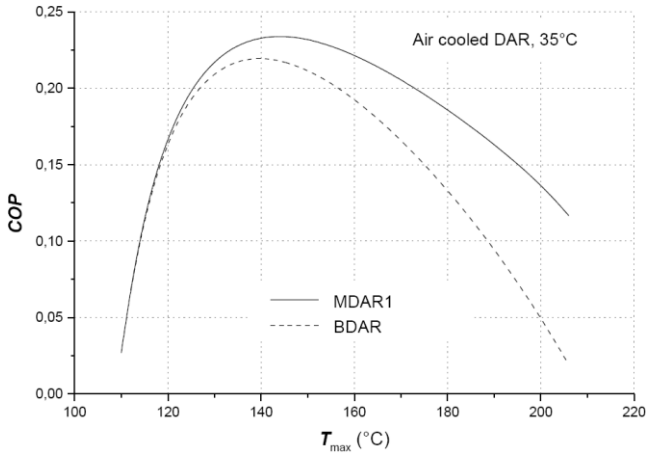

Fig. 7 BHDAR & MHDAR1 COP vs. driving heat temperature

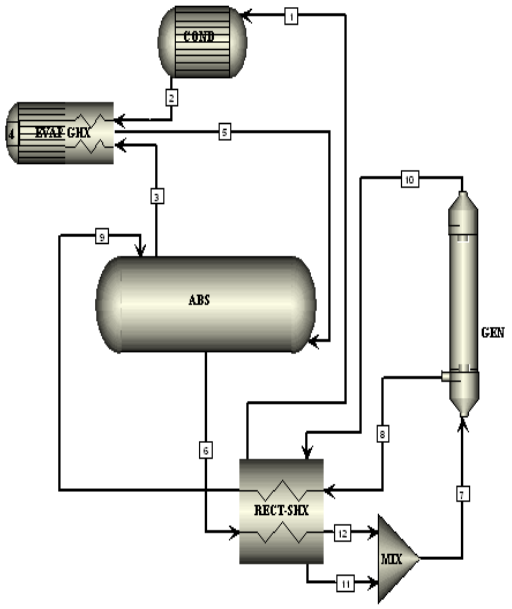

Fig. 8 Circulation patterns of the second enhanced MHDAR2

This second new enhanced configuration of DAR shown in figure 8, is also an extension of the BHDAR. The novel enhancement consist to integration of three-fluid-ways heat exchanger RECT-SHX. When passing through the RECT-SHX the rich solution (6) is preheated simultaneously by the hot weak solution (9) leaving generator and vapor (10) containing some amount of absorbent vapor to be purified.
Resulting rich preheated solution (12) and liquid rectification reflux (11) are then mixed and forwarded to generator.
In the same operating conditions simulation was then performed for the different case study. In the case of 35°C air-cooling medium the three investigated cycles are simulated and compared. Table 3 includes the most important calculation and comparison simulation results for the different studied cycles.
The last figure (Fig. 9) reports the results of the comparison between the basic Platen-Munters hydrogen diffusion absorption refrigerator cycle BHDAR and the two enhanced cycle MHDAR1 and MHDAR2 investigated in this work for varying driving heat temperatures. It shows clearly that the

second modified cycle MDAR2 is more performing. For the air cooled MDAR2 and when the driving temperature reaches a value of 150°C and beyond, the COP is at maximum with a value of 0.37, that is approximately 68% higher than that of the basic diffusion absorption refrigerator.

TABLE II
Heat exchange rates and performances comparison of the HDAR studied cycles

Parameter	**BHDAR**	**MHDAR1**	**MDAR2**
$\dot{Q}_{Evap}$ (W)	1000	1000	1000
$\dot{Q}_{Gen}$ (W)	4554.8	4291.8	3064.5
$\dot{Q}_{Abs}$ (W)	2026.7	3254.	2026.7
$\dot{Q}_{Cond}$ (W)	2037.7	2037.7	2037.7
$\dot{Q}_{Rect}$ (W)	1490.3	-	-
f	4.57	4.83	4.83
COP	**0.22**	**0.233**	**0.33**

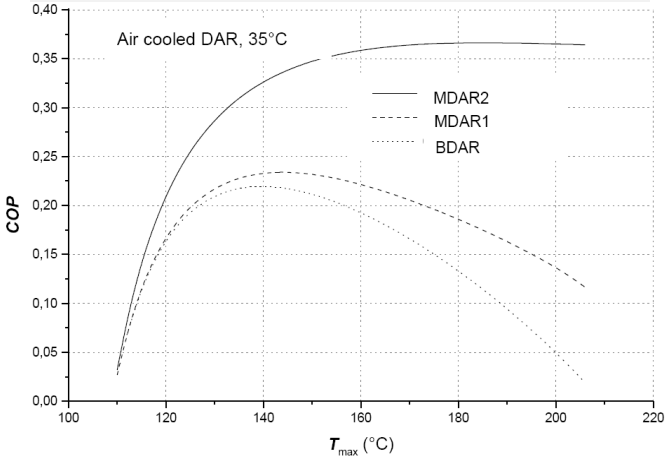

Fig. 9 COP vs. driving temperature for the three studied DAR configurations

VIII. CONCLUSIONS

In this investigation, we proposed two novel enhanced configurations of Hydrogen Diffusion Absorption Refrigeration cycle with different internal heat recovery. This new cycles are then simulated and compared to the basic conventional Pluten-Munters cycle BHDAR.

A thermodynamic model for ammonia-water HDAR cycle is developed and the system performances are analyzed parametrically by computer simulation. The simulation results show that the driving temperature and the absorber efficiency have the largest effect on the *COP* and the minimum evaporation temperature. In the air cooled case, the minimum temperature in the evaporator is about -8 ° C with the absorber effectiveness of 50%; while it drops to -27°C with absorption efficiency of 80%.

The numerical simulation highlights the improved performance of the novel modified cycles. The *COP* of MHDAR2 is at maximum with a value of 0.37, that is approximately 68% higher than that of the basic hydrogen diffusion absorption refrigerator BHDAR (COP=0.22).

REFERENCES

[1] B.C. Von Platen, C.G. Munters. US Patent 1, 685,764, 1928.

[2] A. Koyfman, M. Jelinek, A. Levy, I. Borde, An experimental investigation of bubble pump performance for diffusion absorption refrigeration system with organic working fluids, Applied Thermal Engineering 23 (2003) 1881-1894.

[3] Domestic © 2003, www.dometic.com (formerly known as Electrolux in Europe).

[4] U. Jakob, U. Eicker, D. Schneider, A.H. Taki, M.J. Cook, Simulation and experimental investigation into diffusion absorption cooling machines for air conditioning applications, Applied Thermal Engineering (2007).

[5] A. Zohar, M. Jelinek, A. Levy, I. Brode, Numerical investigation of a diffusion-absorption refrigeration cycle, Int. J. Refrigeration 28(4) (2005) 515–525.

[6] D.A. Kouremenos, A. Stegou-Sagia, Use of helium instead of hydrogen in inert gas absorption refrigeration, International Journal of Refrigeration, 11 (1988), pp. 6-341.

[7] P. Srikhirin, S. Aphornratana, Investigation of a diffusion absorption refrigerator. Applied Thermal Engineering, 22 (2002), pp. 1181-1193.

[8] A. Zohar, M. Jelinek, A. Levy, I. Brode, The influence of diffusion absorption refrigeration cycle configuration on the performance, Applied Thermal Engineering 27 (2007) 2213-2219.

[9] A. Zohar, M. Jelinek, A. Levy, I. Borde, The influence of the generator and bubble pump configuration on the performance of diffusion absorption refrigeration (DAR) system, Int. J. Refrig. 31 (2008) 962-969.

[10] N. Ben Ezzine, R. Garma, M. Bourouis, A. Bellagi, Experimental studies on bubble pump operated diffusion absorption machine based on light hydrocarbons for solar cooling, Renew. Energ. 35 (2010) 464-470.

[11] A. Zohar, M. Jelinek, A. Levy, I. Borde, Performance of diffusion absorption refrigeration cycle with organic working fluids, Int. J. Refrigeration, 32 (2009), pp. 1241–1246.

[12] N. Ben Ezzine, R. Garma, A. Bellagi, A numerical investigation of a diffusion absorption refrigeration cycle based on R124-DMAC mixture for solar cooling. Energy, 5 (2010), 1874-1883.

[13] Q. Wang, L. Gong, J.P. Wang, T.F. Sun, K. Cui, G.M. Chen, A numerical investigation of a diffusion absorption refrigerator operating with the binary refrigerant for low temperature applications, Appl. Therm. Eng., 31 (2011), pp. 1763–1769.

[14] J. Chen, K.J. Kim, K.E. Herold, Performance enhancement of a diffusion-absorption refrigerator, Int. J. Refrigeration 19 (3) (1996) 208-218.

[15] Da-Wen Sun, Comparison of the performance of NH3-H2O, NH3-LiNO3 and NH3-NaSCN absorption refrigeration systems, Energy Conversion Management, 39(5) (1998) 357-368.

[16] R. Saravanan, M.P. Maiya, Experimental analysis of a bubble pump operated H2O-LiBr vapour absorption cooler, Applied Thermal Engineering 23 (2003) 2383-2397.

[17] Y. He, G. Chen, Experimental study on an absorption refrigeration system at low temperatures, International Journal of Thermal Sciences, 46 (2007) 294-299.

[18] I. Borde, M. Jelinek, N.C. Daltrophe, Working fluids for absorption refrigeration systems based on R124 and organic absorbents, Intern. J. Refrig. 20(4) (1997) 256–266.

[19] I. Borde, M. Jelinek, N.C. Daltrophe, Absorption system based on refrigerant R134a, International Journal of Refrigeration, 18(6) (1995) 387–394.

[20] M. Barhoumi, A. Snoussi, N. Ben Ezzine, A. Bellagi, Modelling of the thermodynamic properties of the ammonia –water mixture, International Journal of Refrigeration 27(3) (2004) 271-283.

[21] Kh. Mejbri, N. Ben Ezzine, A. Bellagi, Modélisation numérique des propriétés thermodynamiques du mélange frigorifique ammoniac-eau, Journal de la Société Chimique de Tunisie, 6(2) (2004) 213-228.

[22] G. Alefeld, R. Radermacher, Heat conversion systems, CRC Press, Boca Raton, FL, 1993

[23] N. Ben Ezzine, Kh. Mejbri, M. Barhoumi, A. Bellagi, Thermodynamic analysis and multi-parametric optimisation of double effect absorption chiller , International Journal of Exergy, Vol. 3, N°1, 2006, 68-86.

[24] M. Shacham, Int. J. Num. Methods in Engineering, 23 (1986), pp.1455-1481.